

PHYSICAL MECHANISM FOR THE INTERMEDIATE CHARACTERISTIC STELLAR MASS IN THE EXTREMELY METAL-POOR ENVIRONMENTS

TORU TSURIBE¹ AND KAZUYUKI OMUKAI²

To appear in The Astrophysical Journal Letters.

ABSTRACT

If a significant fraction of metals is in dust, star-forming cores with metallicity higher than a critical value $\sim 10^{-6} - 10^{-5} Z_{\odot}$ are able to fragment by dust cooling, thereby producing low-mass cores. Despite being above the critical metallicity, a metallicity range is found to exist around $10^{-5} - 10^{-4} Z_{\odot}$ where low-mass fragmentation is prohibited. In this range, three-body H_2 formation starts at low ($\sim 100K$) temperature and thus the resulting heating causes a dramatic temperature jump, which makes the central part of the star-forming core transiently hydrostatic and thus highly spherical. With little elongation, the core does not experience fragmentation in the subsequent dust-cooling phase. The minimum fragmentation mass is set by the Jeans mass just before the H_2 formation heating, and its value can be as high as $\sim 10 M_{\odot}$. For metallicity higher than $\sim 10^{-4} Z_{\odot}$, H_2 formation is almost completed by the dust-surface reaction before the onset of the three-body reaction, and low-mass star formation becomes possible. This mechanism might explain the higher characteristic mass of metal-poor stars than in the solar neighborhood presumed from the statistics of carbon-enhanced stars.

Subject headings: hydrodynamics — instabilities — stars: formation, Population II

1. INTRODUCTION

Early generations of stars affect the subsequent evolution of the universe in diverse ways, such as the cosmic reionization and metal-enrichment of the intergalactic medium. In contrast to a number of theoretical attempts to understand their nature in the last decade (e.g., Bromm & Larson 2004; Ciardi & Ferrara 2005), their observational confirmations are thus far extremely limited. Among them, surveys of metal-poor stars in the Galactic halo provide unique tools to catch a glimpse of star formation in very low-metallicity environments in early galaxies (e.g., Beers & Christlieb 2005).

In recent years, hundreds of extremely metal-poor (EMP) stars ($[Fe/H] < -3$) have been found in the halo. A high fraction of them is noticeably enhanced with surface carbon abundance. Such carbon-enhanced extremely metal-poor (CEMP) stars have attracted particular attention in constraining the stellar initial mass function (IMF) in metal-poor environments. Especially, those with *s*-process element enhancement, CEMP-*s* stars, are considered to originate from secondary stars in binary systems. They acquired the surface carbon during the AGB phase of intermediate-mass (several M_{\odot}) primary stars through the binary-mass transfer. Although such carbon enhanced stars are present among population I stars as well (about 1 %), the CEMP-*s* stars make up far higher fraction (about 20 %) of the EMP stars (e.g., Lucatello et al. 2005). Since such a high fraction cannot be accounted for under the same IMF as in the solar vicinity, Lucatello et al. (2005) concluded that the IMF is biased toward higher mass in the early Galaxy. By using more sophisticated stellar evolution models, Komiya et al. (2007) reached similar conclusion. Although there is apparent scarcity of stars in the ultra-metal poor (UMP) range ($-5 < [Fe/H] < -4$) thus far (e.g., Salvadori et al. 2007), three stars has been discovered with $[Fe/H] < -4.8$ and all of them are carbon-enhanced (Christlieb et al. 2002; Frebel et al. 2005; Norris et al. 2007).

Suda et al. (2004) showed that their carbon enhancement can be explained by the binary-transfer hypothesis similar to that for the CEMP stars. Extending the above argument to lower metallicity range, Tumlinson (2007) concluded that the IMF is even more skewed toward massive ones. It is quite natural to conceive that this trend persists also in the UMP range. Moreover, the current lacking of UMP stars might suggest that even less low-mass stars are formed in this range.

Is there any possible mechanism that favors the formation of intermediate-mass stars in these metallicity ranges? In metal-free gas, the first stars are expected to be very massive, more than $100 M_{\odot}$, owing to inefficient fragmentation of dense cores whose mass scale is $\sim 1000 M_{\odot}$ formed at 10^4 cm^{-3} (Bromm, Coppi, & Larson 1999). On the other hand, a slight amount of dust enables fragmentation at higher densities and then low-mass ($< 1 M_{\odot}$) core formation owing to the cooling by dust thermal emission (Schneider et al. 2002, 2003, 2006; Omukai et al. 2005; Tsuribe & Omukai 2006 (paper I)). In this case, although the upper limit of stellar mass is not known, there is no particular reason favoring the formation of intermediate-mass stars.

Here, we propose a physical mechanism that prohibits low-mass star formation in the metallicity range $-5 \lesssim [M/H]_0 \lesssim -4$ despite being above the critical metallicity $[M/H]_{\text{cr}}$ for dust-induced fragmentation.³ This allows transition from intermediate-mass to low-mass star formation mode around the UMP to EMP range provided that a significant fraction of metals are already locked into dust by the time metallicity reaches this value.

2. EFFECT OF H_2 FORMATION HEATING IN LOW-METALLICITY GAS

Fragmentation properties of star-forming cores are largely determined by their thermal evolution. In Figure 1, we show the temperature per unit hydrogen nuclei T/μ ($\propto P/n_H$) for metallicities $[M/H]_0 = -5.5, -4.5$, and -3.5 (solid lines). Also those with $-5 \leq [M/H]_0 \leq -3.8$ are shown by dotted lines

¹ Osaka University, Toyonaka, Osaka 560-0043, Japan; tsuribe@vega.ess.sci.osaka-u.ac.jp

² National Astronomical Observatory of Japan, Mitaka, Tokyo 181-8588, Japan; omukai@th.nao.ac.jp

³ We denote the metallicity in the star-forming gas as $[M/H]_0 \equiv \log(Z/Z_{\odot})$.

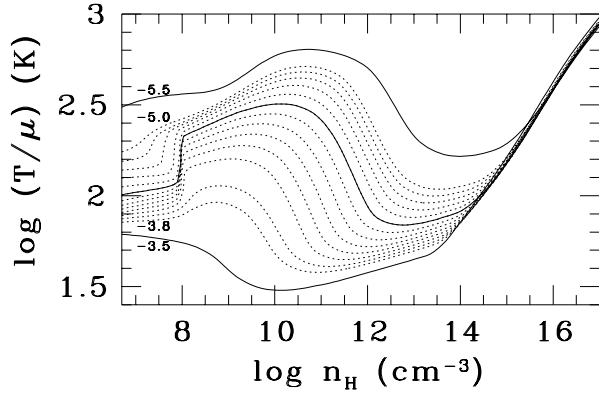


FIG. 1.— The temperature per unit hydrogen nuclei T/μ as a function of number density for metal-poor star-forming cores with $[M/H]_0 = -5.5, -4.5$, and -3.5 (solid). Dust from the pair-instability supernova of $195M_\odot$ is assumed. Those for $[M/H]_0 = -5.5, -5.0, -4.5$ are also shown by dotted lines with an increment of $\Delta[M/H]_0 = 0.1$.

with an increment of 0.1. These are calculated using a one-zone model as in Omukai et al. (2005), except for the dust model, for which we use that produced in the pair-instability supernova of a metal-free $195M_\odot$ star (Schneider et al. 2006). Dust from type II SN gives a similar result (see Schneider et al. 2006). In the case of metallicity $[M/H]_0 \sim -4.5$, a sudden jump in T/μ is present around $n_H \sim 10^8 \text{ cm}^{-3}$, which is caused by heat injection due to three-body H_2 formation (Palla, Salpeter, & Stahler 1983). This temperature jump is observed only in the range $-4.9 \lesssim [M/H]_0 \lesssim -4.0$ (see dotted lines). For lower metallicities (e.g., $[M/H]_0 < -4.9$), the temperature is already high at the density where the three-body reaction begins and the consequence of heat injection is just a gradual increase in temperature. On the other hand, for higher metallicities (e.g., $[M/H]_0 > -4.0$), H_2 formation is almost complete, owing to dust surface reactions. Thus, the three-body reaction plays minor role and the heat injection is small. Only around $[M/H]_0 \sim -4.5$ does heat injection by three-body reaction result in a dramatic temperature increase.

We expect that when the equation of state becomes stiff owing to the H_2 formation heating, a hydrostatic core forms and that it becomes spherical to a high degree. Since an initial elongation of the core of $\gtrsim O(1)$ is required for fragmentation in the dust-cooling phase (paper I), this heating is expected to prevent the subsequent fragmentation. In the following section, we demonstrate that this is indeed the case by way of hydrodynamical calculations.

3. HYDRODYNAMICAL CALCULATIONS

We study the evolution of cloud cores at high densities where the effects of the heating by three-body H_2 formation and cooling by dust are important by performing hydrodynamical calculations. We use a barotropic equation of state (EOS) in Figure 1 for thermal evolution. As in paper I, we choose the self-similar solution with $\gamma \simeq 1.1$ as an unperturbed initial state, to which both non-spherical density/velocity and random-velocity perturbations are added in the same manner as in paper I. The initial amplitude of elongation $\mathcal{E} \equiv a/b - 1$ is taken to be unity, where $a(b)$ is the short (long, respectively) core axis length. In paper I, we started calculation just before the onset of the dust cooling without rotation. Here to see the effect of H_2 formation heating, we start calculation at lower initial number density of $5 \times 10^6 \text{ cm}^{-3}$ at the center. As well as non-rotating cores, in this paper the cores with initial rigid rotation are consid-

ered. Total mass of the cloud is $75M_\odot (T_0/102\text{K})^{3/2}$, where $T_0 = P/(n_H k_B)$ depends on metallicity (Figure 1). We used the smoothed particle hydrodynamics (SPH) based on the Godunov-type scheme (Tsuribe & Inutsuka 1999; Inutsuka 2002) as in paper I, but with implementation of particle splitting by the condition that smoothing length is to be smaller than $1/14$ of the Jeans length. In particle splitting, eight daughter particles are created on the vertices of a cube (Martel et al. 2006) in high density regions. The initial number of SPH particles is $N = 5.2 \times 10^5$. We remark that our method meets the resolution condition for physical fragmentation (e.g., Klein et al. 2004).

3.1. Evolution of A Ultra Metal-Poor Core

The evolution of the core with metallicity $[M/H]_0 = -4.5$ is shown in Figure 2 (a1-a4). The initial core has angular velocity of $0.1\sqrt{4\pi G\rho_c}$, where ρ_c is the initial density at the center. As a result of the prominent H_2 formation heating at $n_H \simeq 10^8 \text{ cm}^{-3}$, the pressure force exceeds gravity. The collapse is almost halted along the short axis of the core while it continues along the long axis. Consequently, the elongation of the core diminishes as can be seen in Figure 3. At this time, the core becomes almost hydrostatic and the accretion shock appears on the surface (Figure 2 (a2)). The core continues to contract owing to accretion of the ambient medium. Although the core becomes elongated during the dust-cooling phase ($n_H \gtrsim 10^{11} \text{ cm}^{-3}$), for $n_H \simeq 3 \times 10^{14} \text{ cm}^{-3}$ the EOS becomes adiabatic and the growth of elongation slows down (see Figure 3). During the dust-cooling phase, elongation grows at the disk formation epoch ($n_H \simeq 10^{14} \text{ cm}^{-3}$). However, with a small value of elongation at the onset of dust cooling, the maximum elongation reaches at most 12 (Figure 2 (a3); Figure 3). We calculated the cases with other values of initial angular velocity ($0.01, 0.03, 0.3$, and $1.0\sqrt{4\pi G\rho_c}$) and found that the maximum value of elongation does not exceed 20 in any case. Since this falls below the critical value for fragmentation ~ 30 (paper I), fragmentation does not occur. We followed the evolution of the core until the early accretion stage and confirmed that it does not fragment (see Figure 2 (a4)). Therefore, the minimum fragmentation mass is set by the Jeans mass before the H_2 formation heating, which is $\sim 10M_\odot$.

3.2. Evolution of Cores with Lower or Higher Metallicities

Here we show that both the cores with $[M/H]_0 = -5.5$ and -3.5 fragment in the dust-cooling phase. We illustrate the case of $[M/H]_0 = -5.5$ with initial angular velocity $0.1\sqrt{4\pi G\rho_c}$ in Figure 2 (b1-b4). For $n_H \gtrsim 10^{11} \text{ cm}^{-3}$ the temperature drops rapidly due to the dust cooling (Figure 1), and the core becomes elongated to a filament (Figure 2 (b2,b3); Figure 3). Although the temperature evolution becomes adiabatic after the core becomes optically thick, for $n_H \gtrsim 3 \times 10^{14} \text{ cm}^{-3}$, the elongation continues to increase owing to inertia. At $n_H \sim 10^{16} \text{ cm}^{-3}$, the elongation attains its maximum of $\mathcal{E} = 49$, which is enough for the filament to fragment (paper I). As seen in Figure 2 (b4), the filament fragments into five pieces and an additional five density peaks are still developing. In the non-rotating case, the maximum elongation is 33 (Figure 3), and two fragments are observed along with additional five growing density peaks. That is, rotation enhances the elongation and promote the fragmentation of the cores. This is because the elongation has longer time to grow during the collapse delayed by rotation.

We also calculated the case of higher metallicity $[M/H]_0 = -3.5$, and found similar evolutionary features, although with larger maximum elongation of $\mathcal{E} = 94$ (Figure 3) even without rotation. The core fragmented into at least seven pieces.

4. CONCLUSION AND DISCUSSION

The dust cooling produces low-mass fragments of star-forming cores with metallicity as low as $[M/H]_0 \lesssim -5$, consistent with previous studies. However, there is a pocket in the metallicity range $-5 \lesssim [M/H]_0 \lesssim -4$, where the low-mass fragmentation is prohibited by sudden heat injection due to the three-body H_2 formation. In this range, the fragmentation mass is $\gtrsim 10 M_\odot$. No low-mass ($< M_\odot$) core is formed, although fragmentation of this intermediate-mass core into a binary is not rejected. Once the metallicity exceeds $[M/H]_0 \sim -4$, low-mass star formation becomes possible by the dust cooling without hindrance by the three-body H_2 formation heating. This provides a physical mechanism for the high characteristic mass (\gtrsim several M_\odot ; Tumlinson 2007) of low-metallicity stars, which is suspected from the observed high frequency of low-metallicity carbon-enhanced stars. In addition, the observed scarcity of ultra metal-poor stars, if confirmed, can be explained. This also means that we need to modify the simplest scenario for the transition in star formation modes in the metal-poor gas; i.e., below a critical metallicity $[M/H]_{cr} (\simeq -6 \dots -5)$ only massive stars are formed while low-mass stars are always formed in gas with metallicities above it (e.g., Salvadori et al. 2006).

In this paper, we showed that H_2 formation on dust grains quenches the sudden heat injection by three-body H_2 formation at a metallicity $[M/H]_0 \sim -4$ and enables low-mass star formation above this metallicity. The range of metallicity $-4.9 \lesssim [M/H]_0 \lesssim -4.0$, where the sudden temperature jump appears, is slightly wider, but similar to the width of the observed gap in the MDF. Although this coincidence is encouraging, it should not be taken at the face value since our calculation still contains uncertain parameters. In particular, the nature of dust, e.g., gas-dust ratio, composition, and size distribution, in the early universe is very uncertain. In the early universe, the dust is assumed to be produced in supernova

events and indeed a signature of dust has been observed in the extinction of high- z quasars and GRBs (Maiolino et al. 2004; Stratta et al. 2007). On the other hand, in the nearby universe, there is no firm evidence for the dust production in supernova remnants (e.g., Bouchet et al. 2006). Even if the dust production is efficient, a significant fraction of it might be destroyed by a reverse shock on the spot (Bianchi & Schneider 2007; Nozawa et al. 2007). In addition, the rate coefficient of three-body reaction rate is still uncertain, in particular, at low temperatures (Flower & Harris 2007; Glover 2007). Considering those uncertainties, we should admit that although our prediction that the heating by three-body reaction prevents low-mass fragmentation in some metallicity range somewhere around $[M/H]_0 \sim -4.5$ remains valid qualitatively, the exact metallicity range where this mechanism works would be altered.

Finally, we discuss effects of rotation. Our result shows that the rotation accelerates the growth of elongation, thereby promoting the fragmentation. This is consistent with the result by Clark, Glover, & Klessen (2007), who showed that, even in the primordial gas, where no fragmentation is observed without rotation, rotating cores can fragment after the formation of rotation supported disks although fragmentation is far less frequent than other cases. In our cases, the core does not fragment in the metallicity range $-5 \lesssim [M/H]_0 \lesssim -4$ even with rotation. Since parameters of the initial cores are not thoroughly surveyed here, some cores might result in fragmentation in this metallicity range. Even so, we expect that the number of such low-mass fragments is smaller than in other range. More studies on the effects of rotation on low-metallicity star formation are awaited.

We thank Simon Glover, Raffaella Schneider and an anonymous referee for comments improving the manuscript. Numerical computations were in part carried out on VPP5000 systems at the CfCA of NAOJ and the Altix 3700 at the Yukawa Insititute (Kyoto). This research was supported in part by Grants-in-Aid from MEXT of Japan (KO;18740117,18026008).

REFERENCES

- Beers, T. C., & Christlieb, N. 2005, *ARA&A*, 43, 531
 Bianchi, S., & Schneider, R. 2007, *MNRAS*, 378, 973
 Bouchet, P., Dwek, E., Danziger, J., Arendt, R. G., De Buizer, I. J. M., Park, S., Suntzeff, N. B., Kirshner, R. P., & Challis, P. 2006, *ApJ*, 650, 212
 Bromm, V. & Larson, R. B. 2004, *ARA&A*, 42, 79
 Bromm, V. & Loeb, A. 2003, *Nature*, 425, 812
 Christlieb, N., Bessell, M. S., Beers, T. C., Gustafsson, B., Korn, A., Barklem, P. S., Karlsson, T., Mizuno-Wiedner, M., & Rossi, S. 2002, *Nature*, 419, 904
 Ciardi, B., & Ferrara, A. 2005, *Space Science Reviews*, 116, 625
 Clark, P. C., Glover, S. C. O., & Klessen, R. S. 2007, *ApJ*, submitted, (preprint arXiv:0706.0613 [astro-ph])
 Frebel, A. et al. 2005, *Nature*, 434, 871
 Flower, D. R. & Harris, G. J. 2007, *MNRAS*, 377, 705
 Glover, S. C. O. 2007, First Star III conference proceedings, arXiv:0708.3086 [astro-ph]
 Inutsuka, S. 2002, *JCoPh*, 179, 238
 Jappsen, A.-K., Glover, S. C. O., Klessen, R. S., & Mac Low, M.-M. 2007, First Star III conference proceedings, arXiv:0708.4363 [astro-ph]
 Klein, R. I., Fisher, R. & McKee, C. F. 2004, *Rev. Mex. AA Ser. Conf.*, 22, 3
 Komiya, Y., et al. 2007, *ApJ*, 658, 367
 Lucatello, S., Gratton, R. G., Beers, T. C., & Carretta, E. 2005, *ApJ*, 625, 833
 Martel, H., Evans, N. J., II, & Shapiro, P. R. 2006, *ApJS*, 163, 122
 Maiolino, R., Schneider, R., Oliva, E., Bianchi, S., Ferrara, A., Mannucci, F., Pedani, M., & Roca Sogorb, M. 2004, *Nature*, 431, 533
 Norris, J. E. 2007, *ApJ*, submitted (preprint arXiv:0707.2657 [astro-ph])
 Omukai, K., Tsuribe, T., Schneider, R. & Ferrara, A. 2005, *ApJ*, 626, 627
 Palla, F., Salpeter, E. E., & Stahler, S. W. 1983, *ApJ*, 271, 632
 Salvadori, S., Schneider, R. & Ferrara, A. 2006, *MNRAS*, submitted (preprint astro-ph/0611130)
 Santoro, F., & Shull, J. M. 2006, *ApJ*, 643, 26
 Schneider, R., Ferrara, A., Natarajan, P., & Omukai, K. 2002, *ApJ*, 571, 30
 Schneider, R., Ferrara, A., Salvaterra, R., Omukai, K., & Bromm, V. 2003, *Nature*, 422, 869
 Schneider, R., Inoue, A. K., Omukai, K. & Ferrara, A. 2006, *MNRAS*, 369, 1437
 Stratta, G., Maiolino, R., Fiore, F., & D'Elia, V. 2007, *ApJ*, 661, L9
 Suda, T., Aikawa, M., Machida, M. N., Fujimoto, M. Y., & Iben, Icko, Jr. 2004, *ApJ*, 611, 476
 Stratta, G., Maiolino, R., Fiore, F., & D'Elia, V. 2007, *ApJ*, 661, L9
 Tsuribe, T. & Inutsuka, S. 1999, *ApJ*, 523, L155
 Tsuribe, T. & Omukai, K. 2006, *ApJ*, 642, L61 (paper I)
 Tumlinson, J. 2007, *ApJ*, 665, 1361

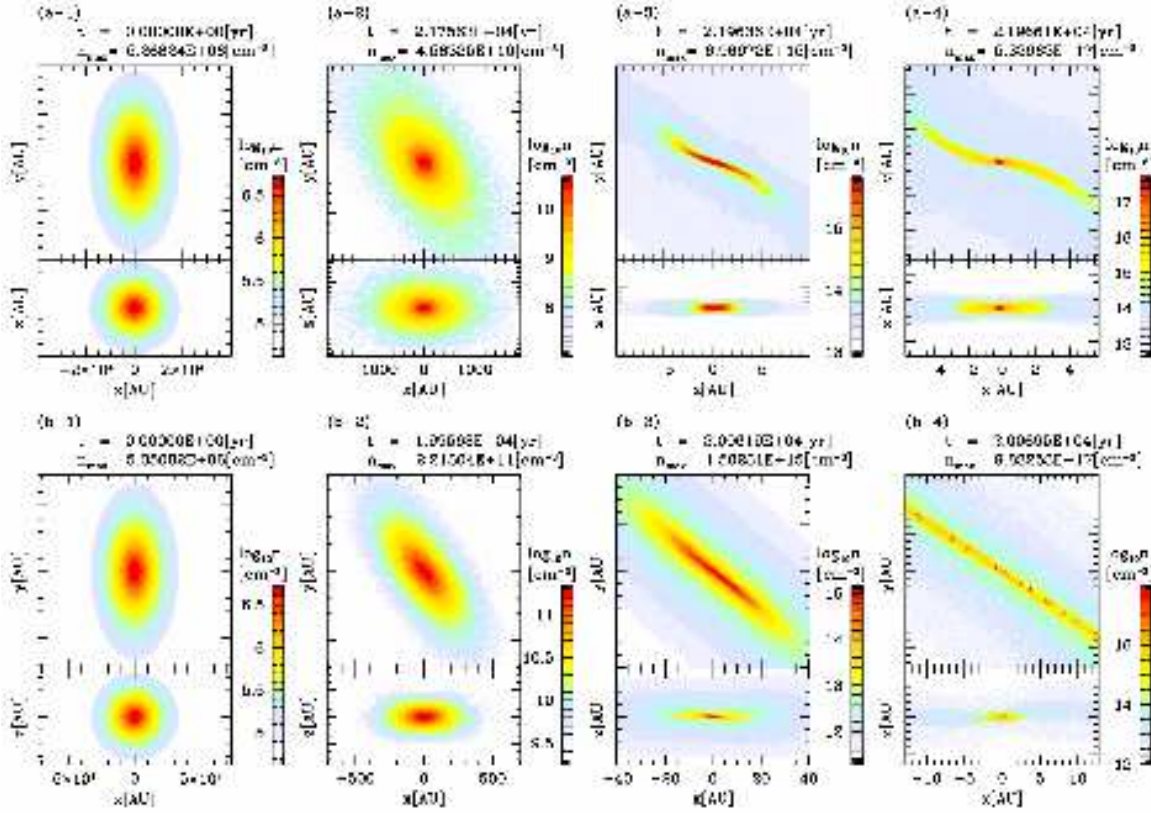


FIG. 2.— Evolution of cores with (a) $[M/H]_0 = -4.5$ and (b) -5.5 . The initial angular velocity is $0.1\sqrt{4\pi G\rho_c}$. Four different stages (panels 1-4) are shown from left to right. Density distributions in the $z=0$ plane (top), and the $y=0$ plane (bottom) are shown in each panel. The panels 1 show the initial states, where the elongation is $\mathcal{E} = 1.0$. The color scale denotes the density in the logarithmic scale. The maximum number density and elapsed time are indicated on the top of each panel.

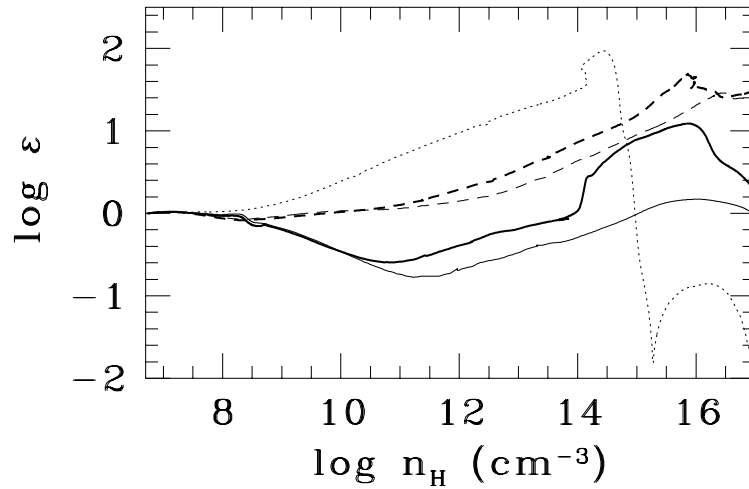


FIG. 3.— Evolution of elongation \mathcal{E} of the cloud cores with metallicity $[M/H]_0 = -5.5$ (dashed) and -4.5 (solid). Thick lines show the case with initial angular velocity $0.1\sqrt{4\pi G\rho_c}$, while thin lines show the cases without rotation, respectively. A non-rotating model with $[M/H]_0 = -3.5$ is also shown by the dotted line. Elongation is calculated for the central region where the density is higher than $1/4$ of the maximum density. The cores with $[M/H]_0 = -5.5$ and -3.5 fragment when their \mathcal{E} 's exceed the critical value ~ 30 . For the core with $[M/H]_0 = -4.5$, owing the decrease of elongation by heating due to H_2 formation ($10^8 - 10^{12} \text{ cm}^{-3}$), the elongation does not reach the critical value in the dust cooling phase.